Journal of the American College of Cardiology Vol. 47, No. 8 Suppl C

Published by Elsevier Inc.
ISSN 0735-1097/06/$32.00
doi:10.1016/j.jacc.2005.11.049

Radionuclide Imaging for the Detection of Inflammation in Vulnerable Plaques

John R. Davies, BSc, MBBS, MRCP,* James H. F. Rudd, PhD, MRCP,†
Peter L. Weissberg, MD, FRCP,* Jagat Narula, MD, PhD, FACC‡
Cambridge, United Kingdom; New York, New York; and Irvine, California

Imaging of atheromatous plaques has traditionally centered on assessing the degree of luminal stenosis. More recently it has become clear that the vulnerable atherosclerotic plaques responsible for the majority of life-threatening syndromes are characterized by high numbers of inflammatory cells and proteins. This has highlighted the urgent need for suitable imaging techniques that can identify and quantify levels of inflammation within atheromatous lesions. Positron emission tomography and single-photon emission computed tomography imaging hold promise in this regard. Tracer compounds capable of assessing macrophage recruitment, foam cell generation, matrix metalloproteinase production, macrophage apoptosis, and macrophage metabolism have been developed and tested in the carotid and peripheral circulation. The identification of inflamed lesions within the coronary circulation, however, remains elusive owing to small plaque size, cardiac and respiratory motion, and lack of a suitable specific nuclear tracer. (J Am Coll Cardiol 2006;47:C57–68) © 2006 by the American College of Cardiology Foundation

Most of the techniques for imaging atherosclerotic lesions have been aimed at providing anatomic detail of plaque size and luminal narrowing. Few techniques are able to provide quantifiable information regarding the cellular, biochemical, and molecular composition of lesions that dictate stability of the plaque. Thus, our ability to identify plaques at risk of rupture and therefore patients at risk of complications such as myocardial infarction and thromboembolic stroke remains limited; however, by labeling tracer compounds that are capable of identifying important cellular or molecular processes with radioactive isotopes (also known as radionuclides), there is the potential to provide clinicians with a powerful imaging tool with which to identify vulnerable plaques, and patients at high risk of atherosclerotic complications. In addition, because of its non-invasive nature, radionuclide imaging could be used to monitor the effects of therapeutic interventions, both established and experimental.

Over the last twenty years it has become clear that inflammatory cells and proteins play a critical role in destabilization of atherosclerotic plaques (1) and thus provide an obvious target for nuclear imaging of the vulnerable lesion. This article aims to review the progress made within this field.

THE PRINCIPLES OF NUCLEAR IMAGING IN RELATION TO IMAGING OF ATHEROSCLEROSIS

Imaging with radionuclide tracer compounds is a multistage process. It begins with production of the radionuclide and its conjugation with a tracer compound. This is followed by administration of the tracer compound to the patient and its subsequent detection by techniques such as single-photon emission computed tomography (SPECT) and positron emission tomography (PET). The raw data collected by the scanner then have to be corrected to account for errors due to attenuation, scatter, random decay events, and dead time, and finally computer reconstruction allows for the production of two-dimensional and three-dimensional topographical images revealing the distribution of the tracer compound within the tissues in the field of view.

The small size of most atherosclerotic lesions and their anatomical proximity to other structures places exacting demands on nuclear imaging systems. This is certainly the case with coronary lesions, which have a cross-sectional area of typically <10 mm^2, are subject to cardiac motion, and lie adjacent to the myocardium, a substrate for "background" tracer uptake. Ideally, tracers for atheroma imaging should bind specifically to plaque constituents and should be rapidly cleared from the circulation to allow for sufficient contrast between the plaque and the blood pool. Uptake in adjacent tissues should also be minimal. Most nuclear imaging studies carried out so far have tended to concentrate on the larger lesions present in carotid, aortic, and iliofemoral arteries. In this article discussion will be limited to those methods that target important inflammatory components of the vulnerable plaque and that have either proved successful or that show promise for the future.

THE BIOLOGY OF PLAQUE INFLAMMATION

Advanced atherosclerotic lesions comprise a lipid-rich core covered by a smooth muscle cell and matrix-rich fibrous cap. The vulnerable plaque, whether it be present in coronary, carotid, or peripheral arteries is typified by an abundance of inflammatory cells and proteins (2–4), all of which provide

From the *Addenbrookes Hospital, University of Cambridge, Cambridge, United Kingdom; †Imaging Science Laboratory, Mount Sinai Hospital, New York, New York; and the ‡University of California-Irvine School of Medicine, Irvine, California. Work of Drs. Davies and Weissberg is supported by grants from the British Heart Foundation. Dr. William A. Zoghbi acted as guest editor.

Manuscript received June 16, 2005; revised manuscript received October 10, 2005, accepted November 16, 2005.

JACC Vol. 47, No. 8 Suppl C
April 18, 2006:C57–68

Abbreviations and Acronyms

CT	= computed tomography
FDG	= fluorine-18–labeled deoxyglucose
HO-CGS 27023A	= ^{123}I-labeled molecule
MCP-1	= monocyte chemotactic protein-1
MDA2	= malondialdehyde-2
MMP	= matrix metalloproteinase
MRI	= magnetic resonance imaging
oxLDL	= oxidized low-density lipoprotein
PET	= positron emission tomography
PS	= phosphatidyl serine
SPECT	= single-photon emission computed tomography
Tc	= technetium
TIA	= transient ischemic attack
WHHL	= Wantanabe heritable hyperlipidemic

potential targets for radionuclide tracers. Macrophages play a central role in the destabilization of atherosclerotic lesions. Circulating monocytes are recruited to atheromatous lesions in response to the expression of adhesion molecules and chemotactic proteins such as monocyte chemotactic protein (MCP)-1 (5). Once recruited, they differentiate into macrophages and ingest oxidized lipoproteins, thereby generating foam cells (6). Foam cells and newly recruited macrophages secrete a host of pro-inflammatory cytokines as well as enzymes such as matrix metalloproteinases (MMP) that breakdown the connective tissue of the fibrous cap resulting in structural changes that reduce its ability to resist the mechanical forces placed upon it by the flowing blood (7). Foam cells in the atherosclerotic lesions frequently exhibit endoplasmic reticular stress, which is associated with phosphatidyl serine (PS) expression on the cell surface, which in turn contributes to foam cell apoptosis (8). Extensive upregulation of caspases is seen in atherosclerotic lesions (9), and overt apoptosis of macrophages is commonly observed in fibrous caps at the site of plaque rupture; apoptosis further augments surface PS expression (10).

Radionuclide tracers have been developed that can identify some of the important pathways associated with plaque instability, such as macrophage recruitment, foam cell formation, matrix breakdown enzymes, macrophage metabolism, and apoptosis (Fig. 1). Table 1 provides a summary of some of the studies that have been carried out.

IMAGING OF MONOCYTE RECRUITMENT

Monocyte chemotactic protein-1 labeled with iodine-125 (^{125}I) has been shown to accumulate selectively in lipid-rich, macrophage-rich regions of experimental atherosclerosis in rabbits where the radiotracer uptake closely correlated with the severity of lesions (11). The ratio of radioactivity in plaque to normal vessel was 6:1. Furthermore, there was a strong correlation between percent injected dose per gram accumulation of ^{125}I-MCP-1 in the atherosclerotic lesions and quantitative estimates of the number of macrophages per unit area ($r = 0.85$, $p < 0.0001$). Encouragingly, plasma clearance of the tracer was also rapid with a clearance half-life of 10 min, suggesting that external imaging of inflamed plaques with MCP-1 tracers might be possible.

At present no in vivo imaging studies using the aforementioned tracer compounds have been published. Therefore, it remains uncertain as to whether this approach to non-invasive external imaging of macrophage recruitment is achievable in vivo in man; however, the importance of macrophage recruitment with regard to plaque instability justifies the ongoing efforts of investigators in this field.

IMAGING OF LIPOPROTEIN PHAGOCYTOSIS AND FOAM CELL GENERATION

Vulnerable lesions are characterized by high levels of low-density lipoprotein accumulation, oxidation, and phagocytosis by plaque macrophages and foam cells. Lipid metabolism therefore provides a suitable target for identifying high-risk plaques.

Oxidized low-density lipoprotein (oxLDL) particles have been successfully radio-labeled, allowing investigators to identify lipid accumulation within macrophages and foam cells present in atheromatous plaques. Iuliano et al. (12) used ^{99m}technetium (Tc)-oxLDL to successfully image symptomatic human carotid lesions in vivo. They found that uptake of ^{99m}Tc-oxLDL by carotid plaques was significantly higher compared with normal carotids ($p = 0.02$). Uptake of ^{99m}Tc-oxLDL above that of the normal carotid artery was observed in 10 of 11 carotid plaques (91%, confidence limits 58.7 to 99.8). No correlation between the degree of stenosis and the target to background uptake ratio was seen.

Given that the clinical utility of radiolabeled autologous oxLDL is likely to be limited owing to the time-consuming preparation process, several groups have synthesized and tested antibody tracers that bind to epitopes on the oxLDL molecule. The majority of studies performed thus far have used radiolabeled malondialdehyde-2 (MDA2), a prototype murine monoclonal antibody that binds to the malondialdehyde epitope on the oxLDL molecule. Experiments in hypercholesterolemic apolipoprotein E null mice and Wantanabe heritable hyperlipidemic (WHHL) rabbits have shown that lipid-rich lesions accumulated approximately 20 times more ^{125}I-MDA2 than normal arterial tissue (13). Immunohistochemistry confirmed co-localization of ^{125}I-MDA2 uptake with macrophage foam cells. In an ex vivo autoradiography study, ^{125}I-MDA2 has been shown to have the capability to track changes in macrophage foam cell density after dietary manipulation (14). Immunohistology revealed that decreased uptake of ^{125}I-MDA2 after dietary plaque regression did not correlate with a decrease in plaque size but was associated with a decrease in macrophage foam cell number, an increase in vascular smooth muscle cells, and a higher collagen content (15). These results suggest that MDA-2 could be used as a marker of plaque stability. Preliminary studies carried out on

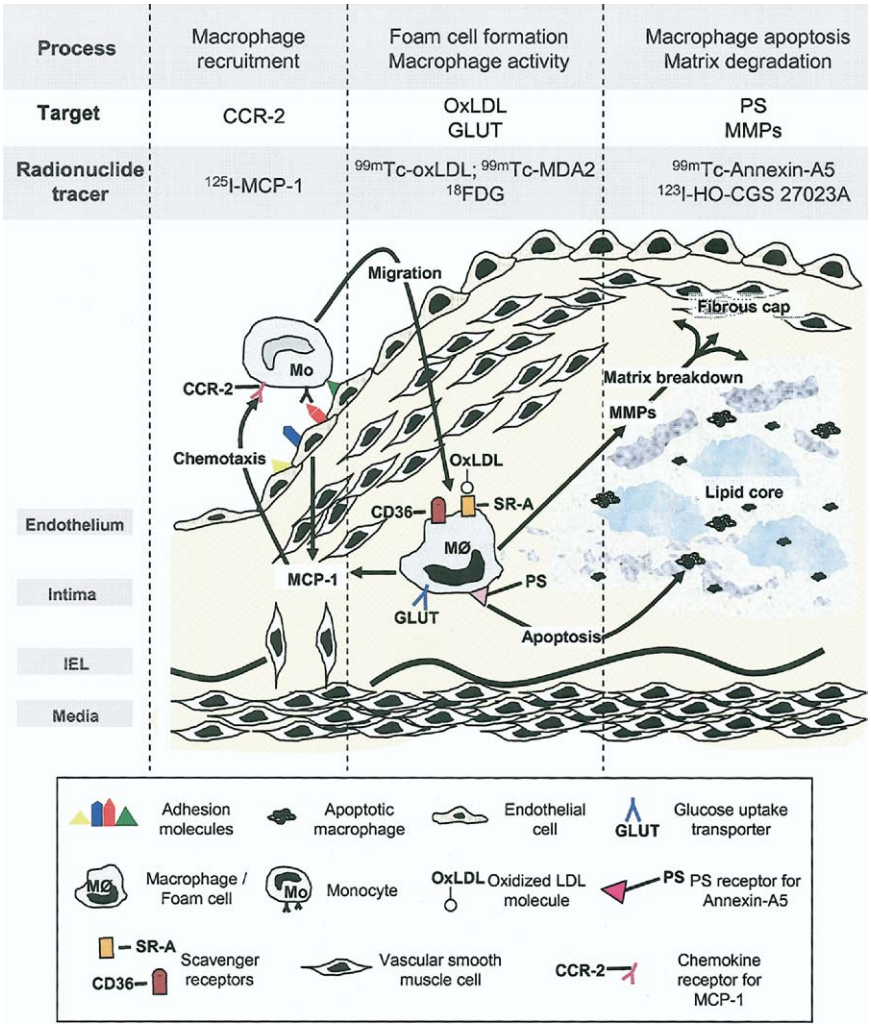

Figure 1. Targets for nuclear imaging of plaque inflammation. Schematic representation of inflammatory cells, molecules, and processes that present potential targets for the identification of vulnerable plaques. CCR-2 = chemokine receptor 2; CD36; cluster differentiation 36; GLUT = glucose uptake transporter; IEL = internal elastic lamina; MCP-1 = monocyte chemotactic protein-1; MMP = matrix metalloproteinase; oxLDL = oxidized low-density lipoprotein; PS = phosphatidyl serine; SR-A = scavenger receptor-A.

WHHL rabbits after intravenous injection of ^{99m}Tc-MDA2 (13) have confirmed the feasibility of in vivo gamma imaging of aortic plaque (Fig. 2); however, a visible signal was only seen in four of seven WHHL rabbits, and no quantification of the in vivo images was attempted. Therefore, the in vivo imaging capability of this technique remains in doubt.

In an attempt to increase the amount of tracer entering the plaque, genetically engineered antibodies against human oxLDL have been synthesized. Their small molecular size should enable higher lesion-to-blood ratios, which should allow for more effective in vivo imaging. In vitro and ex vivo experiments carried out in experimental animal models and on excised human atheroma have given promising results (16), but we will have to await the outcome of in vivo imaging studies before the clinical potential of this tracer can be predicted. Despite the lack of in vivo human data, this approach holds the most promise in terms of imaging and quantifying lipid transport in advanced human lesions.

IMAGING OF PLAQUE MMP

Plaque instability occurs as a result of excessive secretion of MMP enzymes that break down the connective tissue matrix of the plaque. When activated by oxLDL and pro-inflammatory cytokines, macrophages secrete inactive MMP, including interstitial collagenases (MMP-1), gelatinase B (MMP-9), and stromolysins (MMP-3), which are activated in situ by plasmin (17,18). Immunohistochemistry shows that MMP production is predominantly in the vicinity of macrophages in human coronary atherosclerotic lesions (19). Kopka et al. (20) have successfully synthesized a number of synthetic radiolabeled MMP inhibitors that bind to the active zinc(II) ion on a broad spectrum of MMPs. They studied a ^{123}I-labeled molecule (HO-CGS 27023A) in apolipoprotein E null mice that had undergone carotid artery ligation followed by high-cholesterol diet to induce rapid development of atherosclerosis (21). They showed that, after injection of ^{123}I-HO-CGS 27023A, uptake into

Table 1. Radionuclide Tracer Compounds Used to Image Inflammation in Atherosclerotic Lesions

Target Mechanism	Target Cell/Molecule	Tracer	Animal/Human	Successful In Vivo Imaging	Notes
Macrophage chemotaxis	CCR-2	^{125}I-MCP-1	NZW rabbit aorta	NA	Excellent correlation with macrophage number. Fast plasma clearance. Potential candidate for coronary imaging but in vivo studies yet to be reported.
LDL phagocytosis and foam cell generation	LDL	^{123}I-LDL	Human carotid	✓ SPECT	Long plasma half life of tracers necessitates imaging several hours after tracer injection, a problem that compromises clinical utility.
		^{99m}Tc-LDL	Human carotid, ileo-femoral	✓ SPECT	
	oxLDL	^{99m}Tc-oxLDL	Human carotid	✓ SPECT	Rapid plasma clearance c.f. native LDL tracers make it a more promising candidate for in vivo imaging; however, time-consuming tracer production process.
		^{99m}Tc-MDA2	Apo E −/− mouse WHHL rabbit	✓ SPECT	No human studies reported.
MMP activity	MMP	^{123}I-HO-CGS 27023A	Apo E −/− mouse carotid	✓ SPECT	Encouraging pharmacokinetic and in vivo imaging results. Has potential for coronary imaging but no human studies reported so far.
		^{111}In-MMP inhibitor	NZW rabbit aorta	✓ SPECT	
Apoptosis	PS	^{99m}Tc-annexin-A5	NZW rabbit aorta, human carotid	✓ SPECT	Clinical applications in patients with carotid disease. Potential for coronary imaging.
Macrophage infiltration/activity	Autologous-monocytes	^{111}In-monocyte	Human	X	Time consuming tracer production. Unlikely to be used for in vivo imaging.
	Ama	^{131}I-Ama-MoAb	WHHL rabbit aorta	X	Slow plasma clearance—unsuccessful gamma imaging.
	GLUT	^{18}FDG	WHHL + NZW aorta Human coronary, carotid, aorta, and iliac	✓ PET	Clinical potential in patients with carotid disease. Myocardial uptake is likely to make coronary imaging difficult to achieve in a high proportion of patients.

Ama-MoAb = amino malonic acid monoclonal antibody; Apo E −/− = apolipoprotein E null; CCR = chemokine receptor; ^{18}FDG = 18-fluorodeoxyglucose; GLUT = glucose transporter protein; LDL = low-density lipoprotein; MCP = monocyte chemotactic protein; MDA = molondialdehyde; MMP = matrix metalloproteinase; NA = not attempted; NZW = New Zealand White; oxLDL = oxidized low density lipoprotein; PET = positron emission tomography; PS = phosphatidyl serine; SPECT = single photon emission computed tomography; WHHL = Wantanabe heritable hyperlipidaemic.

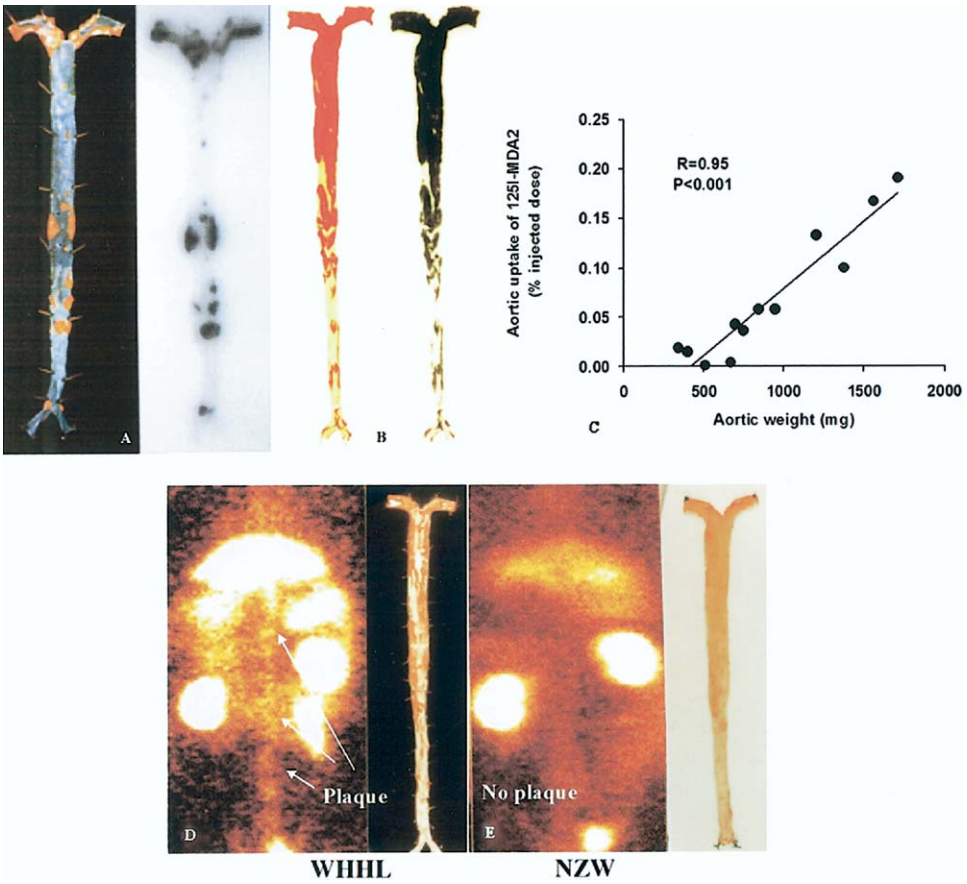

Figure 2. In vivo gamma camera images of experimental aortic atheroma after injection of ^{99m}technetium-malondialdehyde-2 (Tc-MDA2). En-face preparations of Sudan-stained aortas from an apolipoprotein E null (ApoE−/−) mouse **(A)** and a Watanabe heritable hyperlipidemic (WHHL) rabbit **(B)** injected with ^{125}I-MDA2, a murine antibody binding to malondialdehyde–low-density lipoprotein, a model oxLDL epitope. Red color **(left panels in A and B)** represents plaque stained with Sudan IV, and black color **(right panels in A and B)** in the corresponding autoradiograph represents accumulated ^{125}I-MDA2 reflecting the presence of oxLDL. **(C)** shows the relationship of ^{125}I-MDA2 uptake and plaque burden as measured by aortic weight. **(D and E)** represent in vivo imaging of atherosclerotic WHHL **(D)** and non-atherosclerotic New Zealand White **(E)** rabbits with ^{99m}Tc-MDA2. Abbreviations as in Figure 1. Reprinted, with permission, from Tsimikas et al. (13).

lesioned carotid arteries was significantly higher than normal arterial tissue from the contralateral carotid artery and carotid arteries from the sham and control mice (Fig. 3). In addition, pre-dosing mice with unlabeled ligand prevented uptake, indicating a high level of specific binding. Clearance of the tracer from the circulation was rapid, allowing for clear plaque identification on gamma images. Ex vivo gamma counting of arteries from the lesioned mice confirmed uptake into the artery that was not found in the contralateral artery. Micro-autoradiography of the imaged lesions with ^{125}I-HO-CGS 27023A confirmed co-localization of tracer distribution and MMP-9 immunostaining.

A similar broad-spectrum MMP inhibitor radiolabeled with indium-111 has been used to image atherosclerotic lesions in New Zealand White rabbits induced by balloon de-endothelialization of the abdominal aorta and dietary manipulation (22). After intravenous injection of the tracer, gamma camera imaging revealed significantly higher aortic tracer uptake in those on a high-cholesterol diet than in those where the diet was interrupted with normal chow (0.033 ± 0.019% injected dose/g; lesion-to-non-lesion ratio 11:1). In turn, images confirmed that the animals on the interrupted diet regime had higher concentrations of tracer uptake than the control animals that were maintained on a cholesterol-free diet (0.015 ± 0.005% injected dose/g, $p = 0.01$). Threshold analysis of histological sections showed a significantly higher level of immunostaining for MMP in the plaque segments that demonstrated high tracer uptake relative to those with low uptake.

These preliminary observations suggest that MMP might prove to be a suitable target for in vivo imaging of atherosclerosis. Recent reports of ^{11}C and ^{18}F labeling of MMP inhibitors also raise the possibility of PET imaging studies (23). The superior spatial resolution and tracer detection sensitivity of PET would increase the chances of successful coronary plaque imaging with radiolabeled MMP inhibitors.

IMAGING MACROPHAGE STRESS AND APOPTOSIS IN ATHEROSCLEROTIC PLAQUE

Apoptotic cells express PS on their cell surface, and therefore, nuclear imaging of PS expression might identify vulner-

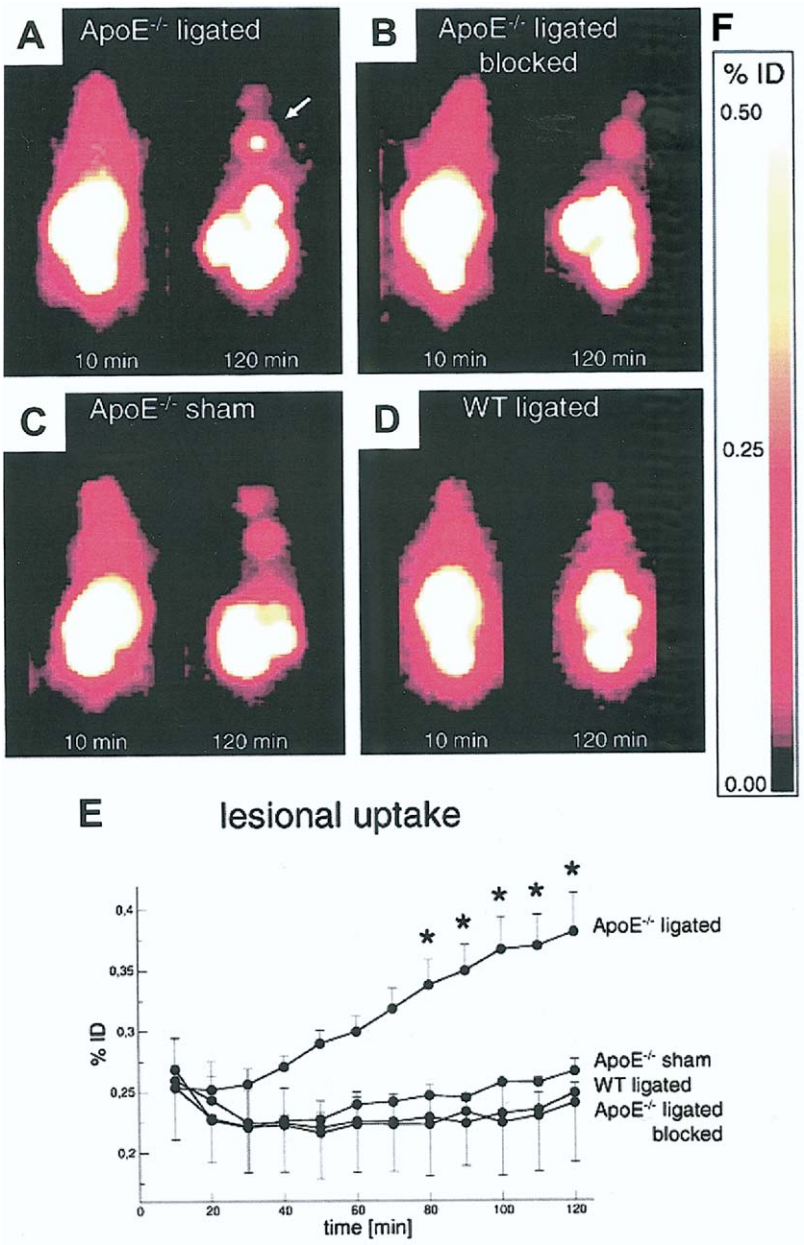

Figure 3. In vivo single-photon emission computed tomography imaging and quantification of matrix metalloproteinase activity in experimental carotid lesions with the tracer, ^{123}I-HO-CGS 27023A. Representative planar images taken 10 min **(left)** and 120 min **(right)** after injection in **(A to C)** apolipoprotein E-deficient (ApoE−/−) mice and **(D)** wild-type (WT) mice 4 weeks after carotid ligation. **(A)** Unblocked; **(B)** after pre-dosing with 6 mmol/l CGS27023A; **(C)** sham-operated; **(D)** WT; **(E)** quantitative uptake of the radioligand in the carotid lesion; and **(F)** tissue uptake over time expressed as % injected dose. *$p < 0.05$ between unblocked and pre-dosed lesional uptake. The signal in the abdominal cavity is non-specific and probably reflects metabolism of the original compound, because there is no inhibition after pre-dosing in all experiments. Reprinted, with permission, from Schafers et al. (21).

able plaques at risk of rupture (24). This expectation might be confounded by the likelihood of PS expression on other constituents of the plaque, such as platelets in overlying thrombus, and on red blood cell membrane remnants in the necrotic core of the lesions; however, given that thrombus and intra-plaque hemorrhage are both associated with plaque vulnerability, this might not present a problem in clinical practice.

Annexin-A5 has a high affinity for the aberrantly expressed PS on the cell surface. Accordingly, ^{99m}Tc-labeled Annexin-A5 has been used for non-invasive imaging of experimental atherosclerotic lesions in rabbits induced by de-endothelialization of the infradiaphragmatic aorta followed by 12 weeks of a high-fat, high-cholesterol diet (24). All animals received radiolabeled annexin-A5 intravenously, and the abdominal aortic atherosclerotic lesions could be observed 2 to 3 h later. Ex vivo images clearly showed uptake of radiotracer corresponding to the lesion distribution within the excised aorta and to tracer uptake seen on the in vivo images. There was no radiotracer uptake in areas

without grossly visible atherosclerotic lesions. As a control, an annexin-A5 mutant that is incapable of binding to PS did not accumulate in the lesions. Similarly, there was no localization of ^{99m}Tc-annexin-A5 in control rabbits without atherosclerotic lesions. Annexin-A5 uptake in atherosclerotic lesions was approximately 10-fold greater than in the non-atherosclerotic aortic wall. The mean percent-injected dose per gram Annexin-A5 uptake in the specimens with lesions correlated with the histologic severity of atherosclerotic lesions; the radiotracer uptake demonstrated that Annexin accumulation predominantly occurred in American Heart Association type IV lesions with only minimal uptake in type II and III lesions. There was a direct relationship of annexin-A5 uptake with macrophage burden ($r = 0.47$, $p = 0.04$) and the magnitude of histologically-verified apoptosis. No association was observed between smooth muscle cell burden and radiotracer uptake ($r = 0.08$, $p = 0.73$).

^{99m}Tc-annexin-A5 has subsequently been used to image atheroma in four patients with carotid vascular disease (25), two of whom had suffered a recent transient ischemic attack (TIA). Tc^{99m}-annexin-A5 uptake was seen in the cervical region in the two patients with recent TIA. No uptake was discernable in the other two patients who had each suffered a TIA more than 6 months before imaging and who were also being treated with high dose statins (Fig. 4). All patients underwent carotid endarterectomy after imaging. The positive Tc^{99m}-annexin-A5 uptake correlated with plaque macrophage content, whereas both patients with negative annexin scans had smooth muscle cell-rich lesions. One of the two patients with recent TIA had a severe lesion on the contralateral carotid but without annexin-A5 uptake. Although these studies suggest that annexin-A5 has promise as an atheroma-imaging agent, it is too early to speculate on its clinical utility. In addition, a lack of anatomical detail on the emission scans makes it difficult to be sure that the uptake is indeed related to atherosclerotic plaque. Since publication of the above studies, annexin-A5 has been successfully conjugated with the positron emitting isotopes, ^{18}F (26) and ^{124}I (27), the latter having been successfully imaged in vivo in an experimental model of hepatocyte apoptosis. This could potentially afford more sophisticated imaging and quantification and allow the detection of apoptosis within coronary lesions.

IMAGING OF PLAQUE MACROPHAGE ACTIVITY WITH FLUORINE-18–LABELED DEOXYGLUCOSE PET

Positron emission tomography, in which paired 511 keV gamma rays are detected by a ring of specialized scintillation detectors, has certain advantages over SPECT. Positron emission tomography can provide 4 to 5 mm resolution compared with 1 to 1.5 cm for SPECT. Positron emission tomography images are derived from the detection of positron-emitting radionuclides, such as carbon-11 and fluorine-18, which can be used to label various biochemical and metabolic substrates. Positron emission tomography agents have the potential to provide a better functional assessment of atherosclerotic plaques than tracers used in conventional nuclear

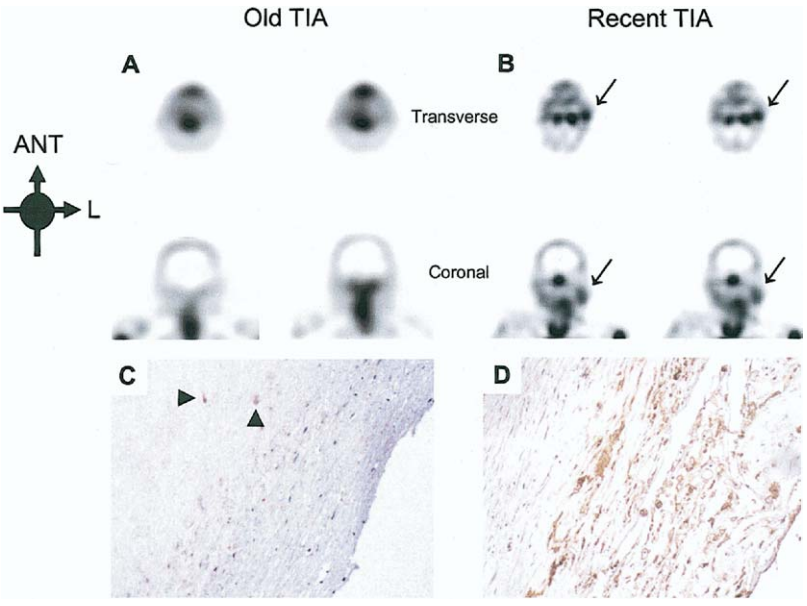

Figure 4. Single-photon emission computed tomography (SPECT) images of unstable atherosclerotic carotid artery lesions obtained with Tc^{99m}-annexin-A5. **(A)** shows transverse and coronal views obtained by SPECT in Patient #1, who had a left-sided transient ischemic attack (TIA) 3 days before imaging. Patient #1 had significant stenoses of both carotid arteries; however, the uptake of Tc^{99m}-annexin-A5 is evident only in the culprit lesion **(arrows)**. Histopathology of an endarterectomy specimen from Patient #1 (**B**, anti–annexin-A5 antibody) shows substantial infiltration of macrophages into the neointima, with extensive binding of annexin-A5 **(brown staining)**. In contrast, SPECT images of Patient #2 **(C)**, who had had a right-sided TIA three months before imaging, do not show annexin-A5 uptake in the carotid region on both sides. Doppler ultrasonography revealed a clinically significant obstructive lesion on the affected side. Histopathological analysis of an endarterectomy specimen from Patient #2 **(D)** shows a lesion rich in smooth-muscle cells, with negligible binding of annexin-A5. ANT = anterior; L = left. Reprinted, with permission, from Kietselaer et al. (25).

imaging, in part as a result of the higher spatial resolution of PET.

Deoxyglucose competes with glucose for uptake into metabolically active cells where it accumulates in proportion to metabolic activity. When labeled with fluorine-18, its accumulation can be imaged and, importantly, quantified by PET. Fluorine-18–labeled deoxyglucose (FDG) PET has been used extensively to estimate myocardial glucose utilization (28) and is becoming the imaging method of choice for identifying tumors (29). The recognition that FDG-PET might have a role in imaging inflammation led to its use in diagnosing and following patients with systemic vasculitides (30,31). In one study of 20 patients with suspected vasculitis, FDG-PET was reported to have 100% positive predictive value and 82% negative predictive value for the diagnosis of vasculitis (31). It has been particularly useful in diagnosing and monitoring the response to treatment in Takayasu's arteritis (32,33). Thus, FDG-PET clearly has the capacity to measure vascular inflammation.

The first studies to show that FDG-PET might have a role in imaging atherosclerosis were performed in cholesterol-fed rabbits. Vallabojosula et al. (34) showed that sufficient FDG was taken up by macrophage-rich atherosclerotic lesions in the aortic arch to be able to image in a conventional human PET scanner. The same group showed that FDG uptake seemed to be related to macrophage content of the plaque. With a similar model, Lederman et al. (35) showed that a positron-sensitive fiber-optic probe placed in contact with the arterial intima could detect high FDG uptake in atherosclerotic segments of the iliac artery. These studies coincided with reports that approximately 50% of patients undergoing FDG-PET for cancer were found, incidentally, also to have high FDG uptake into large arteries (36), assumed to be due to atherosclerosis. Compared with those with no vascular uptake, the patients with high vascular FDG uptake had more risk factors for atherosclerosis (37). These studies strongly suggested that atherosclerotic plaques could be imaged by FDG-PET. Indeed, it is now recognized that atherosclerotic FDG uptake might be misinterpreted as representing the presence of tumor in oncological scans (38).

The first clinical study of FDG-PET imaging of human atherosclerosis was published recently (39). In this study Rudd et al. used autoradiography to demonstrate that when human atherosclerotic plaques are incubated ex vivo, tritiated deoxyglucose are taken up by plaque macrophages but not by surrounding vascular smooth muscle cells or normal vessel. They subsequently undertook FDG-PET scans on eight patients who had experienced a recent TIA and in whom there was angiographic evidence of internal carotid artery stenosis. The FDG-PET images were co-registered with computed tomography (CT) angiograms to ensure that any PET "hot spots" coincided with identified stenotic plaques. They demonstrated FDG accumulation into all eight symptomatic plaques with significantly less FDG uptake into six contralateral asymptomatic plaques (differ-

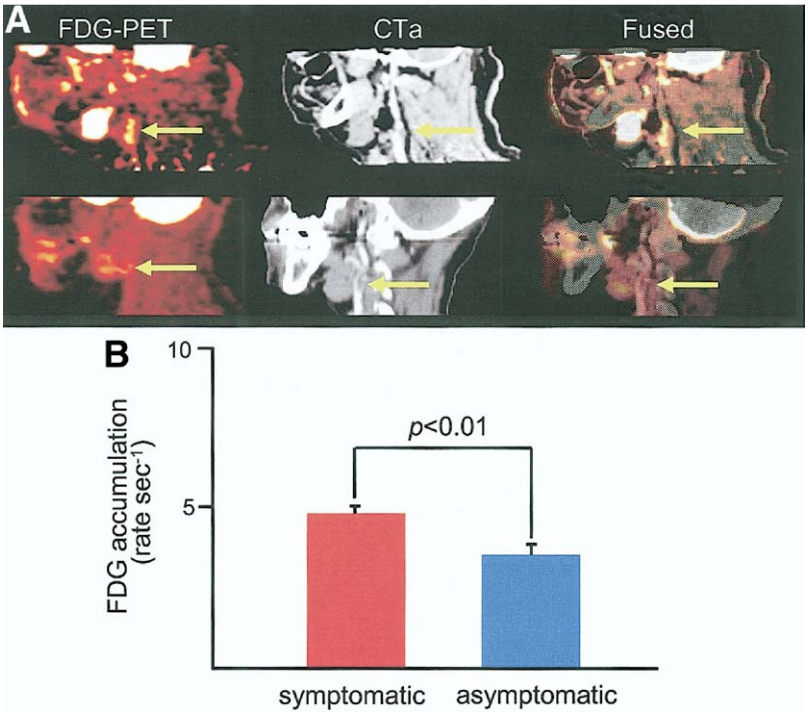

Figure 5. Positron emission tomography (PET) images from patients with unstable carotid disease after administration of fluorine-18–labeled deoxyglucose (FDG). **(A)** FDG-PET **(left column)**, computed tomography (CT) angiography **(middle column)**, and fused **(right column)** images from patient with symptomatic carotid stenosis **(top row)** and contralateral asymptomatic carotid stenosis **(bottom row)**. The **yellow arrows** highlight areas of FDG uptake corresponding to stenotic carotid plaque. **(B)** A graph showing FDG accumulation rate in symptomatic versus asymptomatic carotid plaques. Note that FDG uptake into symptomatic plaque was significantly higher. Modified, with permission, from original figure by Rudd et al. (39).

ence in mean FDG uptake rate of 2.1×10^{-5} s^{-1}, p = 0.005) and no discernable uptake into normal arteries (Fig. 5).

These studies provide proof of principal that FDG-PET can image atherosclerotic plaque inflammation and suggest that it can also quantify plaque inflammatory cell activity. If confirmed, these observations suggest that FDG-PET could be used to identify potentially unstable plaques and to monitor effects of drug therapy on plaque inflammation. Confirmation that FDG-PET can quantify plaque macrophages has come from a recent study in atherosclerotic rabbits that demonstrated a close correlation between FDG uptake and plaque macrophage content ($r = 0.81$, $p < 0.0001$) (40). If FDG-PET is able to identify only those plaques that are most actively inflamed, then it follows that not all plaques should take up significant amounts of FDG. It is becoming clear that this is indeed the case. Three studies have been published recently in which patients with suspected cancer were imaged by both CT and FDG-PET (41–43). Computed tomography measures calcium, which is an almost universal component of atherosclerosis, such that the presence or absence of calcium in the vessel wall is taken to include or exclude the presence of atherosclerosis (44). All studies demonstrated substantial disparity between CT positive and PET positive plaques (Fig. 6); however, these findings are not inconsistent with current understanding of plaque cell biology that would predict that calcification is a consequence of cell death induced by inflammation. Thus FDG uptake indicates current inflammation and therefore potential instability, whereas CT calcification identifies past inflammation and, therefore, relative stability (45).

These studies all suggest that FDG-PET might have an important role to play in identifying vulnerable plaques, although this approach has a number of important limitations that must be overcome if it is to be of wider clinical use. Fluorine-18–labeled deoxyglucose PET provides little or no anatomical resolution and so must be combined and co-registered with another imaging modality to ensure that the PET signal arises from an atherosclerotic plaque and not an adjacent metabolically active structure, such as a lymph node. This will no doubt be facilitated by the wider availability of combined PET/CT scanners; however, any co-registered imaging modality that relies on angiographic principals will be no better at identifying non-stenotic lesions than conventional angiography. Co-registration with high resolution magnetic resonance imaging (MRI), which can characterize non-stenotic as well as stenotic lesions, offers promise for imaging large arteries, such as the carotid. It also has the advantage of not adding to radiation exposure. Our group has recently completed a study in which both FDG-PET and MRI were carried out on a cohort of patients (n = 12) with symptomatic carotid disease, due to undergo carotid endarterectomy (46). Surprisingly, we found that 5 of 12 plaques targeted for endarterectomy had the same degree of FDG uptake as normal vessel wall. In addition, non-stenotic plaques with high FDG uptake were identified in three of these five patients. This study reinforces the advantages of combining FDG-PET with MRI and suggests that this technique might provide a method of selecting appropriate lesions for surgical or percutaneous intervention in patients at risk of stroke. Unfortunately, however, combined MRI/PET scanners are a long way off, and artifacts generated by movement make imaging small vessels, such as the coronary artery, problematic.

The high background uptake of glucose into the myocardium also poses particular problems for the use of FDG-

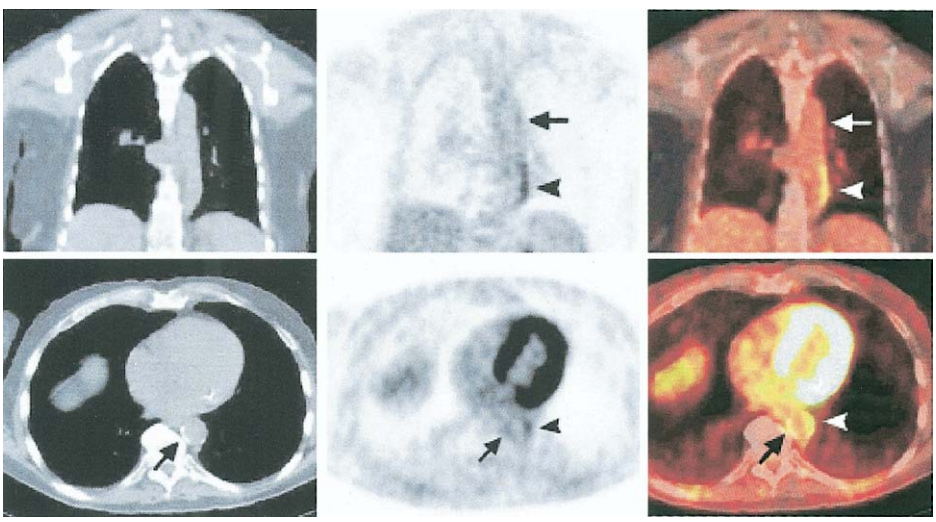

Figure 6. Images obtained by combined positron emission tomography (PET)/computed tomography (CT) machine after administration of fluorine-18–labeled deoxyglucose (FDG) in patients with aortic atheroma. **Top row:** coronal CT **(left)**, FDG-PET **(middle)**, and fused **(right)** images. There is no calcium present in the aortic wall on CT. On the PET and fused images grade 1 **(arrows)** and grade 3 **(arrowheads)**, FDG uptake can be seen in the aortic wall. **Bottom row:** transaxial CT **(left)**, FDG-PET **(middle)**, and fused **(right)** images. The CT image shows marked calcification present on the medial side of the descending aorta **(arrow)**, which on the FDG-PET and fused images demonstrates grade 1 FDG uptake **(arrows)** indicating mild inflammation. Grade 3 FDG uptake is also seen on the lateral side of descending aorta **(arrowheads)** indicating a higher level of inflammation in this segment of non-calcified vessel wall. Modified, with permission, from Tatsumi et al. (42).

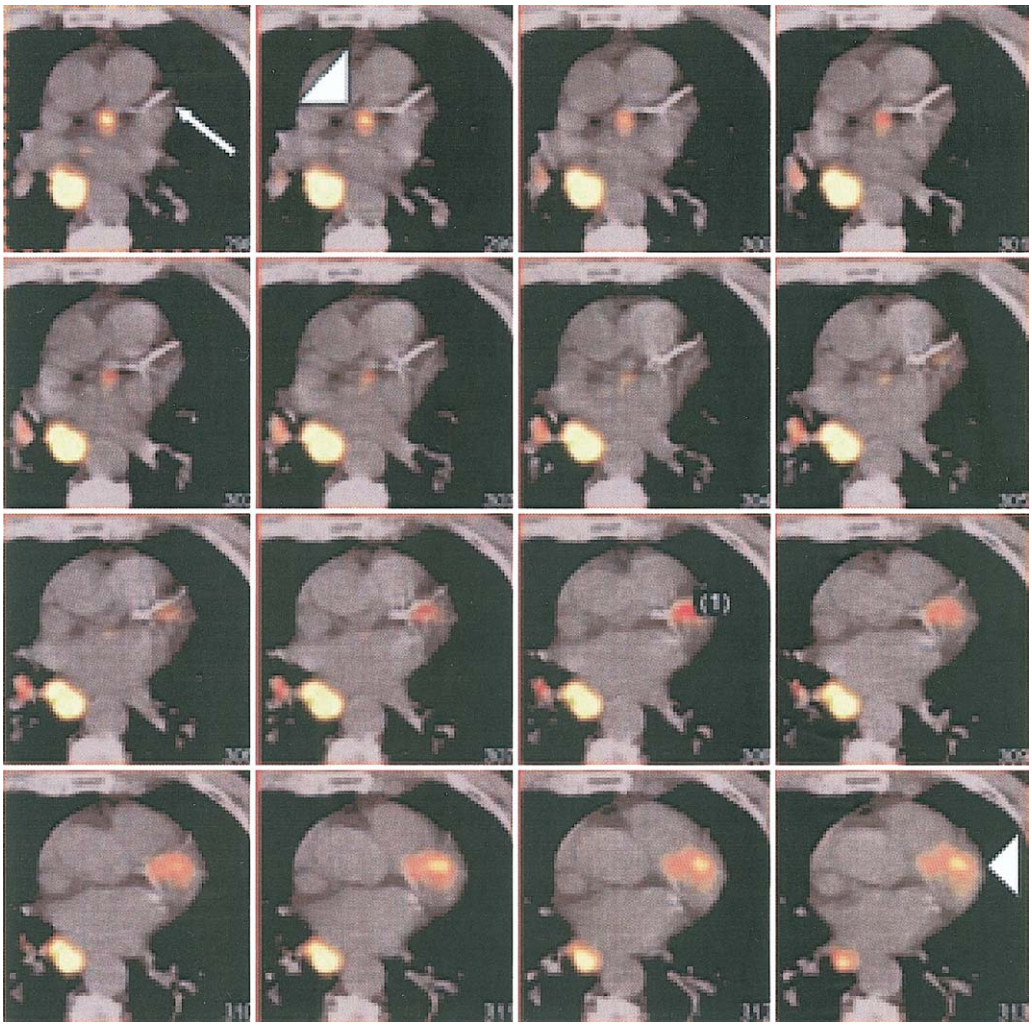

Figure 7. Images from combined positron emission tomography (PET)/computed tomography (CT) scanner showing coronary fluorine-18–labeled deoxyglucose (FDG) uptake. Fused PET/CT images show contiguous transaxial slices through heart. Inflammation **(arrowheads)** is present proximal and distal to the calcified left anterior descending artery **(arrow)**. A tumor sits adjacent to esophagus. Reprinted, with permission, from Dunphy et al. (43).

PET to image coronary atheroma. Despite this, Dunphy et al. (43) have been able to identify FDG uptake in coronary arteries of oncological patients from images obtained from a combined PET/CT scanner (Fig. 7). Coronary FDG uptake was found to be most often proximal and multifocal, which agrees with autopsy studies that coronary inflammation occurs at multiple sites simultaneously (47). Myocardial and hepatic FDG uptake, however, did prevent evaluation of coronary arteries in approximately one-half of the patients studied, and therefore in the future the use of pre-imaging beta-blockade might be necessary to suppress myocardial uptake (48). Despite these results, coronary atheroma imaging will probably be better achieved either with a more macrophage-specific ligand than FDG or by labeling other plaque-specific ligands with positron emitters. Finally, if PET is to be used to monitor changes in plaque composition over time, then the technique will have to be refined to limit radiation exposure.

CONCLUSIONS

Until recently, imaging technology for atherosclerosis has focused almost entirely on defining anatomic obstructions to flow; however, advances in our understanding of the cell biology that leads to clinical events in atherosclerosis have highlighted a clear need for imaging techniques that can provide information about plaque composition. Imaging and quantification of inflammation within atherosclerotic plaques remain important goals with respect to identification and treatment of vulnerable plaques both in the carotid circulation where there is a correlation with stroke risk and in the coronary vasculature where plaque rupture often leads to myocardial infarction and/or death. Although the different approaches described previously do hold promise, no large in vivo prospective trials have been carried out, and unless time, effort, and finance is aimed in the direction of nuclear imaging, we are unlikely to find a suitable

non-invasive method for coronary imaging in the near future. At the present time FDG-PET seems to be the most promising technique for identifying inflamed lesions in the peripheral and carotid circulation. The superior spatial resolution of PET, along with the anatomical co-registration demonstrated by Rudd et al. (39) and Ben Haim et al. (41), increases the potential for imaging plaque inflammation and allows for more sophisticated levels of quantification, such as calculation of plaque glucose metabolic rate; however, FDG-PET is unlikely to provide the answer for non-invasive coronary plaque imaging unless FDG uptake in the adjacent myocardium can be adequately suppressed. Annexin-A5 and MMP tracers are not taken up by the healthy myocardium and therefore could be used for coronary imaging, although they will need to be labeled with positron emitting radionuclides in order to use the superior imaging and quantification capabilities of PET, and anatomical co-registration—for example with multislice CT images—would be necessary to localize tracer uptake to particular coronary segments. The problem of cardiac and respiratory motion will also need to be addressed, and this is likely to be done by using a combination of respiratory and electrocardiographic gating. Hopefully the future will bring further advances in both tracer and detector technologies that will make non-invasive coronary plaque imaging a reality. For now, nuclear imaging of inflammation within atherosclerotic plaques remains in the research domain.

Reprint requests and correspondence: Dr. Peter L. Weissberg, Division of Cardiovascular Medicine, Box 110, Level 6 ACCI, Addenbrookes Hospital, Hills Road, Cambridge CB2 2QQ, United Kingdom. E-mail: weissbergp@bhf.org.uk.

REFERENCES

1. Ross R. Atherosclerosis—an inflammatory disease. N Engl J Med 1999;340:115–26.
2. Davies MJ. Stability and instability: two faces of coronary atherosclerosis. The Paul Dudley White Lecture 1995. Circulation 1996;94: 2013–20.
3. Golledge J, Greenhalgh RM, Davies AH. The symptomatic carotid plaque. Stroke 2000;31:774–81.
4. Libby P, Geng YJ, Sukhova GK, Simon DI, Lee RT. Molecular determinants of atherosclerotic plaque vulnerability. Ann N Y Acad Sci 1997;811:134–42.
5. Rosenfeld ME. Leukocyte recruitment into developing atherosclerotic lesions: the complex interaction between multiple molecules keeps getting more complex. Arterioscler Thromb Vasc Biol 2002;22:361–3.
6. Vainio S, Ikonen E. Macrophage cholesterol transport: a critical player in foam cell formation. Ann Med 2003;35:146–55.
7. Libby P, Geng YJ, Aikawa M, et al. Macrophages and atherosclerotic plaque stability. Curr Opin Lipidol 1996;7:330–5.
8. Tabas I. Apoptosis and plaque destabilization in atherosclerosis: the role of macrophage apoptosis induced by cholesterol. Cell Death Differ 2004;11 Suppl 1:S12–6.
9. Chen J, Mehta JL, Haider N, Zhang X, Narula J, Li D. Role of caspases in Ox-LDL-induced apoptotic cascade in human coronary artery endothelial cells. Circ Res 2004;94:370–6.
10. Kolodgie FD, Narula J, Burke AP, et al. Localization of apoptotic macrophages at the site of plaque rupture in sudden coronary death. Am J Pathol 2000;157:1259–68.
11. Ohtsuki K, Hayase M, Akashi K, Kopiwoda S, Strauss HW. Detection of monocyte chemoattractant protein-1 receptor expression in experimental atherosclerotic lesions: an autoradiographic study. Circulation 2001;104:203–8.
12. Iuliano L, Signore A, Vallabajosula S, et al. Preparation and biodistribution of 99m technetium labeled oxidized LDL in man. Atherosclerosis 1996;126:131–41.
13. Tsimikas S, Palinski W, Halpern SE, Yeung DW, Curtiss LK, Witztum JL. Radiolabeled MDA2, an oxidation-specific, monoclonal antibody, identifies native atherosclerotic lesions in vivo. J Nucl Cardiol 1999;6:41–53.
14. Tsimikas S, Shortal BP, Witztum JL, Palinski W. In vivo uptake of radiolabeled MDA2, an oxidation-specific monoclonal antibody, provides an accurate measure of atherosclerotic lesions rich in oxidized LDL and is highly sensitive to their regression. Arterioscler Thromb Vasc Biol 2000;20:689–97.
15. Torzewski M, Shaw PX, Han KR, et al. Reduced in vivo aortic uptake of radiolabeled oxidation-specific antibodies reflects changes in plaque composition consistent with plaque stabilization. Arterioscler Thromb Vasc Biol 2004;24:2307–12.
16. Shaw PX, Horkko S, Tsimikas S, et al. Human-derived anti-oxidized LDL autoantibody blocks uptake of oxidized LDL by macrophages and localizes to atherosclerotic lesions in vivo. Arterioscler Thromb Vasc Biol 2001;21:1333–9.
17. Lendon CL, Davies MJ, Born GV, Richardson PD. Atherosclerotic plaque caps are locally weakened when macrophages density is increased. Atherosclerosis 1991;87:87–90.
18. Galis ZS, Sukhova GK, Lark MW, Libby P. Increased expression of matrix metalloproteinases and matrix degrading activity in vulnerable regions of human atherosclerotic plaques. J Clin Invest 1994;94:2493–503.
19. Narula J, Virmani R, Zaret B. Radionuclide imaging of atherosclerotic lesions. In: Braunwald E, Dilsizian V, Narula J, editors. Atlas of Nuclear Cardiology. Philadelphia, PA: 2003:217–35.
20. Kopka K, Breyholz HJ, Wagner S, et al. Synthesis and preliminary biological evaluation of new radioiodinated MMP inhibitors for imaging MMP activity in vivo. Nucl Med Biol 2004;31:257–67.
21. Schafers M, Riemann B, Kopka K, et al. Scintigraphic imaging of matrix metalloproteinase activity in the arterial wall in vivo. Circulation 2004;109:2554–9.
22. Kolodgie FD, Edwards S, Petrov A, et al. Noninvasive detection of matrix metalloproteinase upregulation in experimental atherosclerotic lesions and its abrogation by dietary modification (abstr). Circulation 2001;104:694.
23. Zheng QH, Fei X, Liu X, et al. Synthesis and preliminary biological evaluation of MMP inhibitor radiotracers [11C]methyl-halo-CGS 27023A analogs, new potential PET breast cancer imaging agents. Nucl Med Biol 2002;29:761–70.
24. Kolodgie FD, Petrov A, Virmani R, et al. Targeting of apoptotic macrophages and experimental atheroma with radiolabeled annexin V: a technique with potential for noninvasive imaging of vulnerable plaque. Circulation 2003;108:3134–9.
25. Kietselaer BL, Reutelingsperger CP, Heidendal GA, et al. Noninvasive detection of plaque instability with use of radiolabeled annexin A5 in patients with carotid-artery atherosclerosis. N Engl J Med 2004; 350:1472–3.
26. Toretsky J, Levenson A, Weinberg IN, Tait JF, Uren A, Mease RC. Preparation of F-18 labeled annexin V: a potential PET radiopharmaceutical for imaging cell death. Nucl Med Biol 2004;31:747–52.
27. Keen HG, Dekker BA, Disley L, et al. Imaging apoptosis in vivo using 124I-annexin V and PET. Nucl Med Biol 2005;32:395–402.
28. Phelps ME, Hoffman EJ, Selin C, et al. Investigation of [18F]2-fluoro-2-deoxyglucose for the measure of myocardial glucose metabolism. J Nucl Med 1978;19:1311–9.
29. Strauss LG, Conti PS. The applications of PET in clinical oncology. J Nucl Med 1991;32:623–48.
30. Meller J, Strutz F, Siefker U, et al. Early diagnosis and follow-up of aortitis with [(18)F]FDG PET and MRI. Eur J Nucl Med Mol Imaging 2003;30:730–6.
31. Bleeker-Rovers CP, Bredie SJ, van der Meer JW, Corstens FH, Oyen WJ. F-18-fluorodeoxyglucose positron emission tomography in diagnosis and follow-up of patients with different types of vasculitis. Neth J Med 2003;61:323–9.

32. Webb M, Chambers A, Al Nahhas A, et al. The role of 18F-FDG PET in characterising disease activity in Takayasu arteritis. Eur J Nucl Med Mol Imaging 2004;31:627–34.
33. Andrews J, Al Nahhas A, Pennell DJ, et al. Non-invasive imaging in the diagnosis and management of Takayasu's arteritis. Ann Rheum Dis 2004;63:995–1000.
34. Vallabhajosula S, Machac K, Knesaurek J. Imaging atherosclerotic macrophage density by positron emission tomography using F-18 fluorodeoxyglucose (FDG) (abstr). J Nucl Med 1996;37 Suppl:38P.
35. Lederman RJ, Raylman RR, Fisher SJ, et al. Detection of atherosclerosis using a novel positron-sensitive probe and 18-fluorodeoxyglucose (FDG). Nucl Med Commun 2001;22:747–53.
36. Yun M, Yeh D, Araujo LI, Jang S, Newberg A, Alavi A. F-18 FDG uptake in the large arteries: a new observation. Clin Nucl Med 2001;26:314–9.
37. Yun M, Jang S, Cucchiara A, Newberg AB, Alavi A. 18F FDG uptake in the large arteries: a correlation study with the atherogenic risk factors. Semin Nucl Med 2002;32:70–6.
38. Hanif MZ, Ghesani M, Shah AA, Kasai T. F-18 fluorodeoxyglucose uptake in atherosclerotic plaque in the mediastinum mimicking malignancy: another potential for error. Clin Nucl Med 2004;29:93–5.
39. Rudd JH, Warburton EA, Fryer TD, et al. Imaging atherosclerotic plaque inflammation with [18F]-fluorodeoxyglucose positron emission tomography. Circulation 2002;105:2708–11.
40. Ogawa M, Ishino S, Mukai T, et al. (18)F-FDG accumulation in atherosclerotic plaques: immunohistochemical and PET imaging study. J Nucl Med 2004;45:1245–50.
41. Ben Haim S, Kupzov E, Tamir A, Israel O. Evaluation of 18F-FDG uptake and arterial wall calcifications using 18F-FDG PET/CT. J Nucl Med 2004;45:1816–21.
42. Tatsumi M, Cohade C, Nakamoto Y, Wahl RL. Fluorodeoxyglucose uptake in the aortic wall at PET/CT: possible finding for active atherosclerosis. Radiology 2003;229:831–7.
43. Dunphy MP, Freiman A, Larson SM, Strauss HW. Association of vascular 18F-FDG uptake with vascular calcification. J Nucl Med 2005;46:1278–84.
44. Budoff MJ, Shavelle DM, Lamont DH, et al. Usefulness of electron beam computed tomography scanning for distinguishing ischemic from nonischemic cardiomyopathy. J Am Coll Cardiol 1998;32:1173–8.
45. Weissberg PL. Noninvasive imaging of atherosclerosis: the biology behind the pictures. J Nucl Med 2004;45:1794–5.
46. Davies JR, Rudd JHF, Fryer TD, et al. Identification of culprit lesions after transient ischaemic attack by combined [^{18}F]fluorodeoxyglucose positron emission tomography and high resolution magnetic resonance imaging. Stroke 2006. In press.
47. Spagnoli LG, Bonanno E, Mauriello A, et al. Multicentric inflammation in epicardial coronary arteries of patients dying of acute myocardial infarction. J Am Coll Cardiol 2002;40:1579–88.
48. Tokita N, Zanzonico P, Dunphy M, et al. Suppression of physiological myocardial fluorodeoxyglucose uptake (abstr). J Am Coll Cardiol 2004;43 Suppl A:337A.